THE AMERICAN SOCIETY OF MECHANICAL ENGINEERS
345 E. 47 St., New York, N.Y. 10017

92-GT-41

BREAK

A Combustor Diffuser of Annular Configuration Suitable for Industrial Gas Turbines

R. C. ADKINS*
Department of Gas Turbines
ABB Power Generation Ltd.
Baden, Switzerland

and

A. C. BENIM, P. C. ESCHER, J. HELLAT, W. M. KOENIG
R & D Thermal Machinery Dept.
ABB Turbo Systems Ltd.
Baden, Switzerland

ABSTRACT

A pre-combustor diffuser, suitable for outboard annular combustors has been successfully demonstrated. The diffuser, which incorporates a 180 degree bend and practicalities such as support struts, was shown to produce a pressure recovery and flow stability which would be superior to most inline annular diffusers. Guidelines for the design of such diffusers are discussed.

NOMENCLATURE

A	area
AR_0	overall area ratio
C_{bl}	bend pressure loss coefficient
C_p*	optimum pressure coefficient
OGV	outlet guide vane
P_{bl}	bend pressure loss
R_m	mean radius in bend
v	velocity
v_{mean}	mean velocity
α	kinetic energy coefficient
ρ	density

INTRODUCTION

The trend in large industrial gas turbines is towards annular combustors in order to meet the requirements of compactness, efficiency and low emissions of exhaust gas pollutants. These combustors are often located outboard of the turbomachinery silhouette in order to provide the extra space needed for combustion efficiency and to facilitate maintenance. A further benefit, that of reduced shaft length, can also be obtained but this depends upon the ability to both decelerate and turn the airstream in the pre-combustor diffuser. If this cannot be achieved then the penalty of diffuser pressure loss on engine efficiency is well known. However, there is an effect which can be even more detrimental to the operation of modern engines which occurs when the diffusor flow is unstable.

Lean burn combustors are used in order to obtain low NOx emissions and inevitably these operate closer to the weak extinction limit. This makes them significantly more sensitive to fluctuations in airflow than earlier combustors. For instance, a momentary reduction in air supply will richen the combusting gases and so raise the temperature, leading to the generation of a disproportionately higher quantity of NOx. Alternatively, a momentary increase in air flow will weaken the combusting mixture and create pockets of gas in which weak extinction will occur. This results in both a pulsation in pressure and the release of CO. By these means minor flow fluctations, originating in the diffuser can be amplified into significant pressure pulsations inside the combustor and the release of pollutants.

The pre-combustor diffuser has therefore assumed a greater importance in this type of engine and its design is made more difficult by the need to both turn and diffuse the flow. It was the early recognition of this problem which prompted ABB to conduct studies on a number of new diffuser configurations and one of these studies forms the basis of this paper.

The diffusor/combustor configuration chosen for the study is shown in Figure 1 in which a diffuser is separated into two stages by a 180 degree bend. Another feature of this arrangement is the removal of bleed air, for engine cooling purposes, at the start of the bend. Further deceleration of the remainder of the air is then achieved in the second diffuser stage before it is delivered to the combustor dome and burners. The study was made realistic by linking it to a previous engine design study. In this way

* Visiting engineer from Cranfield Institute of Technology, U.K.

Presented at the International Gas Turbine and Aeroengine Congress and Exposition
Cologne, Germany June 1-4, 1992

typical dimensional constraints, flow disturbances such as support struts and non uniform flow conditions at diffuser inlet could be correctly included.

The unusual layout of the new diffuser dictated that the design be based upon fundamental considerations rather than on experience gained from any previous similar diffusers. Accordingly the study was divided into three parts:

1) Basic design
2) Evaluation using computational fluid dynamics
3) Evaluation by aerodynamic testing of a scale model

BASIC DESIGN

Requirements

The dimensional constraints were taken from an engine design study and these are presented here as fractions of the inner wall radius at diffuser inlet. The following details are also of particular interest:

1) The compressor delivery was inclined at an angle of 5 degrees towards the engine axis.
2) The diffuser commenced at the exit plane of the compressor outlet guide vanes. Here the ratio of outer radius:inner radius = 1.105.
3) The profile of the inner wall of the first stage diffuser was defined by the engine main shaft assembly.
4) The conical outer wall of the diffuser second stage was determined by the inner casing of the combustor.
5) Diffuser length was controlled by the axial distance between the compressor and the various flow passages and supports upstream of the turbine.
6) The engine specifications required a cooling air flow of 11.7% to be taken from the diffuser in the region of the bend.
7) The mean velocity at diffuser exit was required to be less than 26% of that at inlet.
8) Ten struts, carrying axial load were to be located in the bend section of the model.
9) The diffuser pressure loss was to be less than 1.5% of the total pressure at diffuser inlet (when the inlet Mach number was 0.3).
10) The design was to be mechanically simple.

Philosophy

This was influenced mainly by the requirements of mechanical simplicity and low pressure loss. The section most likely to generate pressure loss is the 180 degree bend where pressure loss, P_{b1}, is given by:

$$P_{b1} = C_{b1} \times \text{(bend approach dynamic pressure)}$$

where C_{b1} is the coefficient of loss.

The loss coefficient is dependent upon bend geometry but this led to a problem because no relevant data was found for annular bends of the type required for this application. Use was therefore made of empirical data taken from two-dimensional bends of constant cross-sectional area and of large aspect ratio (width:height = 8:1). Such data is given in Figure 2 and shows that C_{b1} is dependent upon the fraction, bend height to mean radius, w/R_m, and that this fraction must be kept to a value of less than 1.0 in order to avoid large pressure loss coefficients and hence flow separation and instabilities.

The above relationship indicated the possibility of a conflict between obtaining low values of C_{b1} and low values of approach dynamic pressure. If the area increase in the first stage of the diffuser is made appreciable, in order to reduce dynamic pressure, then there is less space for turning the flow and C_{b1} then becomes large. A parametric study was therefore made in order to determine whether there was an optimum area ratio of the first stage diffuser which would lead to a minimum pressure loss in the bend. This study showed that the bend loss continued to reduce with reduction in diffuser area ratio. Clearly some diffusion is essential in the first diffuser stage in order to produce the target exit velocity. It was therefore decided to compromise and adopt a value of bend fraction, w/R_m, which would permit as much first stage diffusion as possible without causing flow separation from the bend.

DESIGN

Preliminary calculations

The profile of the shaft casing was given by a table of co-ordinates. It was necessary to describe these by a polynomial equation for use in the marching procedure which is described later in this section. An equation of degree 5 was required in order to obtain the correct level of accuracy.

A further equation describing the inner profile of the combustor casing was also derived.

Diffusor First Stage

This is the section reaching from compressor outlet guide vanes to the 180 degree bend and was to be canted radially inwards with an initial angle of 5 degrees. The inner wall of this stage was defined by the shaft casing and so it was only necessary to design the outer wall of the passage in a manner that would optimise the flow. This was accomplished in two parts. The first part maintained a constant cross sectional area for a distance equal to one-half of the compressor OGV chord. This has the benefits of enabling any wakes generated by the OGV's to close and also gives an opportunity for any flow distortion generated by the compressor to mix out. Furthermore, it avoids any unwanted upstream influence of the diffuser upon flow in the compressor.

The second part of this first stage diffuser was designed using the "G parameter," described fully by Adkins (1983, 1990). Here "G" is a non dimensional pressure gradient defined as a ratio of axial to transverse pressure gradients. The design process can be described briefly by the following steps:

1) Estimate the overall area ratio, AR_0, of the two stage diffuser.
2) Use the value of AR_0 to calculate a value for G from an empirical equation given by Adkins (1983), (which was derived from conical, Cp^* diffusers). Here $G = [0.915\,(AR_0)^{1.424} - 1]^{-0.5}$
3) Using one wall of the diffuser (the shaft casing), which was defined in the engine project design study, develop the second wall in such a manner that "G" is kept constant down the length of the diffuser. A step by step, or marching procedure, is used for this.

Cooling Aperture

The aperture was located so that it would face the oncoming flow, at a position just upstream of the 180 degree bend, and so benefit from the stagnation pressure in this region. Following ingestion through the aperture the cooling air could then be diffused further while on route to its various destinations.

The aperture area was made 12.9% of the total duct area, proportionally larger than the cooling air fraction (11.7% of total) that it was to ingest in order to compensate for boundary layer blockage.

Bend Section

As previously mentioned, the empirical data used for the design was taken from two-dimensional bends of constant cross sectional area (and hence constant height). Annular bends, however, cannot conform to both these constraints simultaneously because of the change in radius from the engine axis and so in this design it was the area that was kept constant.

Diffuser Second Stage

The design procedure was similar to that used for the first stage. The same value of 'G', derived from the overall area ratio, remained appropriate. The passage differed, however, because the absence of outlet guide vanes obviated the need for a length of duct with constant cross-sectional area. A further difference was that the outer annulus wall was given by the combustor casing and so here the task was to develop the inner wall of the diffusing passage.

Annular Projection

The basic shape of the annular projection was developed automatically during the design of the two stages of the diffuser.

Iteration

On completion of one cycle of the design procedure the calculated overall area ratio was compared with the estimated one, AR_0. If the comparison was not satisfactory (to within a value of 0.1), then the process was repeated as necessary, using revised values for the estimated area ratio. The iteration process was aided by a suite of computer programmes, specially written for the task, which included both the above marching procedure and the design of the bend.

After convergence was achieved on the overall area ratio the diffuser length was checked, in the event of this length being excessive the lengths of the two specified diffuser walls were reduced by an equal amount. Afterwards the overall area ratio was re-estimated and the above interation process repeated until a satisfactory overall length was achieved.

Leading Dimensions

On satisfactory completion of the iteration process the leading dimensions were found to be as follows for the first stage of the diffuser:

- Area ratio = 2.13:1
- ratio; length/inlet height = 16.05

The diffuser overall:

- Area ratio (geometric) = 3.38
- ratio; length/inlet height = 36.37

COMPUTATIONAL STUDY

As previously implied, the design was of a speculative nature because of the unknown performance of the annular bend and any reaction that it could have with the diffuser stages, both upstream and downstream. It was therefore decided to predict the flow behaviour using computational fluid dynamics before proceeding any further. A three dimensional fluid flow code, Harwell-FLOW3D (Burns et al., 1988), was used where the mathematical model is based upon a body-fitted, non-orthogonal discretization scheme and a pressure correction method for the solution of the Navier-Stokes equations. This was used in conjunction with a suitable turbulence model for closure of the computations, the Reynolds stress model was chosen for present purposes.

The prediction was simplified by assuming that the flow was incompressible, which was reasonable since the inlet Mach number was 0.3, and by excluding the ten support struts so that the flow could be treated as axisymmetric.

A velocity distribution, typical of flows at compressor exit, and a turbulence intensity of 4% with a mixing length of 5% of the channel width were used as boundary conditions at diffuser inlet and a fine grid was used to ensure computational accuracy. All solutions were tested for grid independence and satisfactory numerical convergence (assumed after the mass source convergence term was equal to or less than 0.1%).

The study was conducted in two parts. The first examined the performance of the first stage diffuser up to the start of the bend. The bend was not included in this model and exit conditions were obtained by extending the annular duct at a constant cross-section, for a distance of three annulus heights, downstream of the diffusing passage. The grid (with dummy cells for computational convenience) consisted of 122 x 40 x 3 cells.

The second study included both the diffuser stages and the bend. A grid of 200 x 40 x 3 cells was used for this computational calculation.

Postprocessing was performed using Harwell-OUTPROC (Jackson et al., 1988) which produces 2-D sections of the flows, either in monochrome or colour, and in contour or vector format.

The computations predicted that there would be no flow separation and that the diffuser performance would be satisfactory. The computations gave sufficient confidence for the experimental study to proceed and some of the predicted values are compared with the experimentally determined data in a later section.

AERODYNAMIC TEST

The scale of the diffuser model was sized to give an inlet Mach number of 0.3 when using an available compressed air supply. It was manufactured from high quality, fine grain wood and was of modular construction in order to both simplify modifications and to facilitate velocity traversing at various stations down the diffuser. Ten struts were equidistancially positioned in the bend to both simulate the effect of the struts and to guarantee the concentricity of the inner and outer second stage contour as in the large machine diffuser.

The model was fed from a metered air supply leading to a settling chamber and a smooth annular nozzle (of contraction area ratio 22:1) into the diffuser inlet duct. This was an annular passage of constant diameter and had a ratio of lenght to annulus height of 17.7:1 in order to generate a radial velocity profile which was typical of engine compressor exits, see Figure 3. The diffuser model exhausted directly to atmosphere and so it was anticipated that static pressures in the bend region would be slightly sub-ambient. Accordingly, provision was made to assist the extraction of cooling air from an annular slit located on the interstage bend.

Relevant parameters at diffuser inlet were as follows:

- Ratio of inner to outer diameter at diffuser inlet = 0.9127
- Reynolds number = 2.74×10^5 (based on hydraulic diameter)
- Reynolds number = 2.4×10^6 (based on inlet length)

The modular construction facilitated operation of the model at various stages of completion. In this way velocity profile at inlet and after the first diffuser stage could be measured in addition to the profile at exit of the completed diffuser. This technique avoided the permanent inclusion of total pressure rakes which would otherwise have interfered with the overall pressure recovery. Static pressure measurement were taken from wall taps located on both walls of the two diffuser stages and at six different locations around the circumferences.

All static pressure signals were taken through a computer controlled, Scanni valve system and measured using a 70 mbar (1 psig) pressure transducer, with an accuracy to within 0.1% of the full scale reading. Measurements of air mass flow were assessed using a calibrated orifice and were obtained to within an accuracy of 0.2%.

Diffuser pressure recovery was assessed from a datum inlet plane located upstream of the juncture between axial and canted flow, at a distance equal to one annulus height. The level of equality of measurements taken at this location from both the inner and outer walls confirmed that this distance was sufficient to avoid interference from streamline curvature.

RESULTS

All the following data are taken from the diffuser operating with a nominal inlet Mach number of 0.3 and a bleed rate of 11.7% of the inlet flow. The values of static pressure recovery coefficient, C_p, are defined by:

$$C_p = \frac{\text{static pressure rise}}{0.5 \cdot \rho \cdot v_{mean}^2}$$

where pressure rise is assessed from diffuser inlet plane and v_{mean} = velocity derived from mass flow, density and area.

Values of kinetic energy coefficient, α, are also given for the various velocity profiles in order that the given values of C_p can readily be adapted into other, corrected, forms if prefered. Here α is defined by:

$$\alpha = \frac{\int v^3 \cdot dA}{v_{mean}^3 \cdot A}$$

where A is the area.

Radial velocity profiles were measured at three circumferential locations, namely at 60, 150 and 300 degrees to the top dead centre.

Diffuser Inlet Conditions

These were measured at the end of the annular inlet section after the diffuser had been removed. They are therefore independent of any upstream influence that the diffuser may otherwise have imposed. Radial velocity profiles were measured at the three specified circumferential locations and these were found to be sensibly identical and so are presented as the one profile shown in Figure 4. The value of kinetic energy flux parameter, α was found to be 1.0975.

Diffuser First Stage

The model was designed especially to enable tests on the diffuser first stage to be made without the addition of the bend and second stage diffuser. In this situation it simply exhausted its flow directly through the test cell air extractor which was located sufficiently far downstream in order to avoid aerodynamic interference.

The measured value of C_p was 0.635 which compared well with the ideal theoretical value of 0.779 (derived solely from the area ratio). The resulting diffuser effectiveness of 81.5% was considered to be quite satisfactory when compared with the performance of other annular diffusers. Trace recordings, taken from the pressure transducers confirmed that flow stability was good.

The radial velocity profiles, measured at three circumferential locations, again were sensibly identical. This profile is given together with that predicted using FLOW3D in Figure 5 where a useful similarity can be observed between the two. Both profiles show a slightly inboard peak with values of α as follows:

- Computationally predicted value = 1.479
- Experimentally measured value = 1.363

These values represent the excess kinetic energy (dynamic pressure) present in the flow over and above that of one-dimensional flow where the value of α would have been unity. They therefore suggest that the failure of the diffuser to achieve a value of effectiveness of 100% originates mainly from the increase in flow distortion between inlet and exit rather than from any pressure loss due to friction.

Bend section

No flow measurements were taken in this section as the instrumentation that would have been required for this was beyond the scope of the present study. Use was therefore made of FLOW3D which, in this instance, predicted the flow without the presence of support struts. As such it was limited more to a qualitative than a quantitative role. An enlargement of the velocity vectors in the bend section, while computed as part of the complete diffuser, is presented in Figure 6. This has proved to be very useful in understanding the high performance of the complete diffuser. Features worthy of note are as follows:

1) The peak velocity at exit of the first stage diffuser is now close to the outer wall, on the inside of the bend. Clearly this shift is due to the influence of the bend upon flow upstream. The low velocities at the outer wall of the bend suggest that static pressures in this region would be high and so would provide a good location for the extraction of coolant air.
2) No flow separation is indicated, this is important in terms of flow stability and low pressure loss.
3) The low velocities around the outer wall of the bend indicate that skin frictional losses on this long exposed surface will be only minmimal.

4) High velocities on the inner wall of the bend will oppose flow separation. The relatively short length of exposed surface here should not generate any significant pressure loss due to skin friction.
5) The steep radial gradient in velocity across the bend generates significant Reynolds stresses within the flow which transport energy towards the outer wall, thereby preventing flow separation. It can also be assumed that the turbulence associated with these Reynolds stresses will be of small scale and that it is convected into the second stage of the diffuser where it assists with the diffusion process.

In reality, flow round the bend section would be more complex than that predicted here due to the presence of the support struts. The static pressure gradient across these struts, when coupled with the lack of radial equilibrium in velocity, produced by the strut boundary layers, will generate strong flows transverse to the main stream. These transverse, or secondary flows, will therefore redistribute the mass flux in the second stage diffuser.

Second Stage Diffuse (Overall Performance)

Pressure recovery of the diffuser second stage is included in the performance of the diffuser overall. Although this configuration also exhausted to the test cell and extractor system the unconventional arrangement dictated that the flow at exit would be partly obstructed by the inlet plenum and that it would have to be turned radially outwards. Accordingly, space was included in the design in order to locate the flow turning at some distance away from the diffuser exit to avoid interference with the exit pressure field. The adequacy of this space was confirmed by the closeness of static pressure measurements, taken from both walls at diffuser exit, to the ambient pressure.

The overall pressure recovery coefficient of the complete diffuser system was 0.833 compared with the ideal one-dimensionally derived value of 0.912. From these figures it can be shown that the loss is 0.1053.

Figure 7 shows that the radial velocity profiles measured at the overall diffuser exit vary slightly with circumferential position, presumably due to the influence of the secondary flows generated by the support struts. All three profiles are fairly flat and have a value of α close to unity, indicating in this case that the difference between the measured and ideal values of C_p is due to losses rather than profile distortion. The computed velocity distribution agrees reasonably with the measured distributions. A possible source of difference is that no support struts were included in the computational model.

The high level of flow uniformity at diffuser exit is a most unusual and welcome feature, particularly as it is accompanied by a high level of pressure recovery. Also of interest is the remarkable improvement in flow uniformity between the end of the first stage and the final exit. This indicates that the turbulence generated in the bend region (and also possibly the secondary flows), have assisted in diffusing the flow over the annular cross-section without a significant loss in stagnation pressure, thereby making the diffuser/bend combination very effective.

CONCLUSION

The tests have shown that a 180 degree, annular bend can be successfully incorporated into a pre-combustor diffuser without the use of turning vanes or other complications. Operation of the diffuser with realistic impedences such as support struts, air bleed-off and a non-uniform distribution of velocity at inlet has also been demonstrated.

The pressure recovery of the diffuser (C_p = 0.833) was higher than would normally be expected from a typical, in line annular diffuser when operating in similar circumstances. The improved performance is accredited to the influence of the bend in generating high Reynolds stresses and turbulence which then accelerated the diffusion process in the second stage of the diffuser.

No modification was required to the original design of this diffuser and this fact supports the use of the "G" parameter and computational modeling by FLOW3D as design tools.

ACKNOWLEDGEMENTS

The authors wish to thank their colleagues who assisted with the project, particularly in the manufacture, instrumentation and operation of the test rig. They are also indebted to ABB Power Generation Ltd. for permission to publish.

REFERENCES

Adkins, R.C., 1983, "A Simple Method For Designing Optimum Annular Diffusers," ASME Paper No. 83-GT-42.

Adkins, R.C., and Wardle, M.H., 1990, "A Method For The Design Of Optimum Annular Diffusers Of Canted Configuration," Journal of Engineering for Power [to be published], ASME Paper No. 90-GT-52.

Burns, A.D., Jones, I.P. Kightley, I.R., and Wilkes, N.S., 1988, "HARWELL-FLOW3D, Release 21," Harwell, U.K.

Jackson, C.P. and Winters, K.H., 1988, "A Guide to Post-Processing Using the TGIN Language," Harwell, U.K.

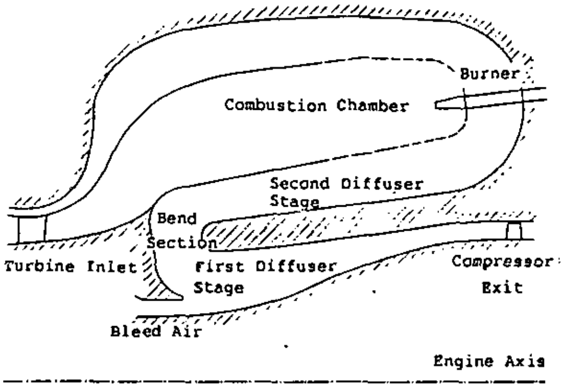

Fig. 1 Scheme of the Annular Two-Stage Diffuser-Combustor Arrangement

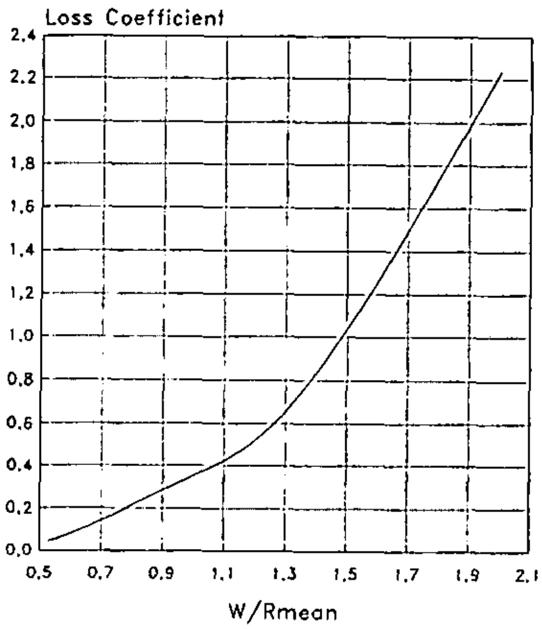

Fig. 2 Dependency of Loss Coefficient from the Related Bend Height

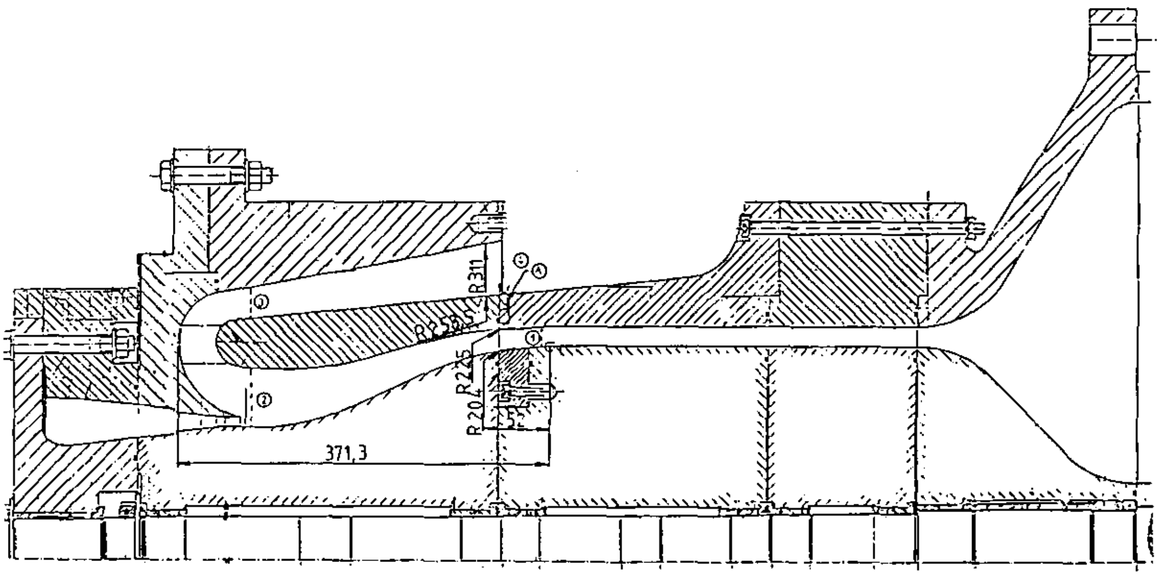

Fig. 3 Cross Section of the Scale Model

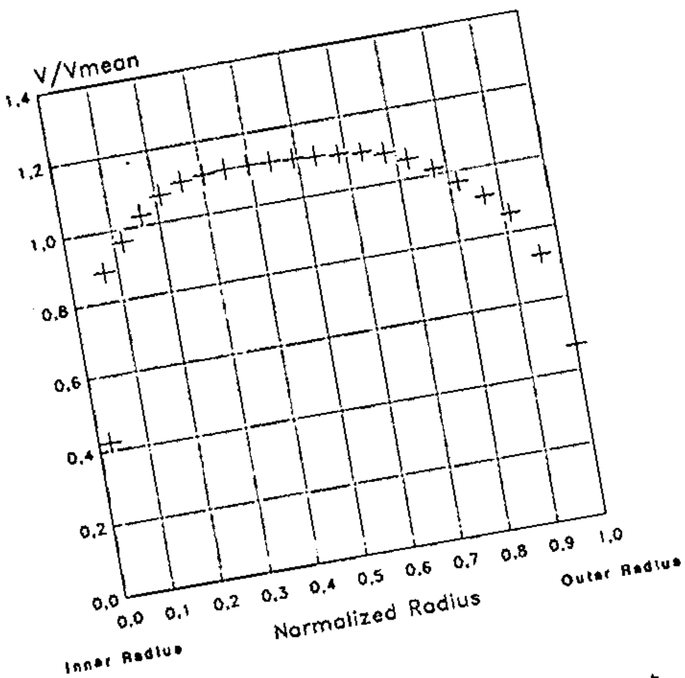

Fig. 4 Measured Velocity Distribution at the Diffuser Inlet

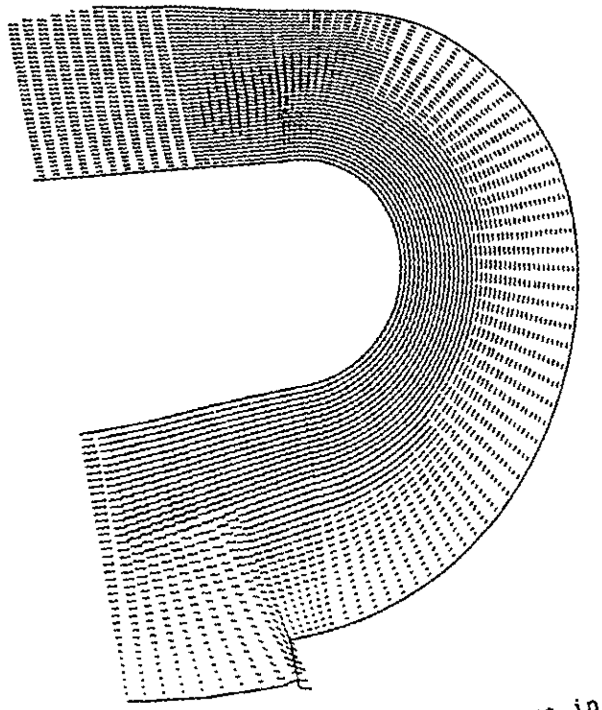

Fig. 6 Computed Velocity Vectors in the Bend Section by FLOW3D

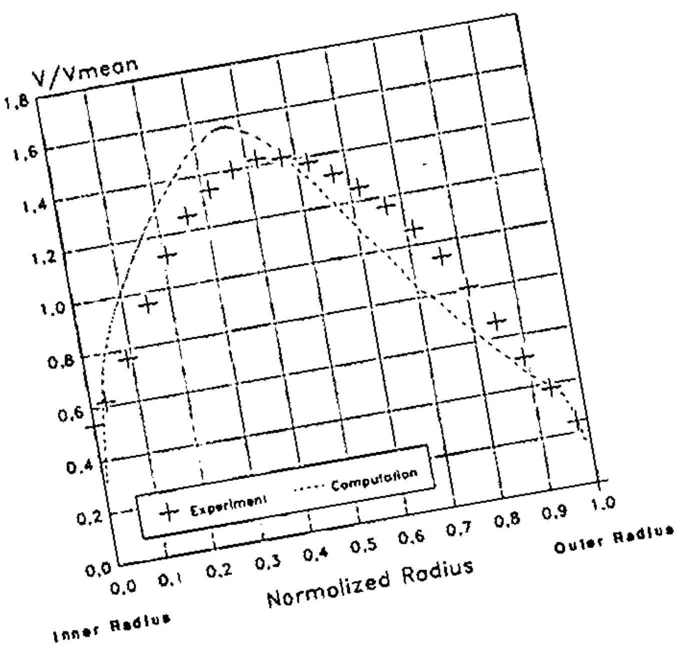

Fig. 5 Comparison of Measured and Calculated Velocity Distributions at the Exit of the First Diffuser Stage

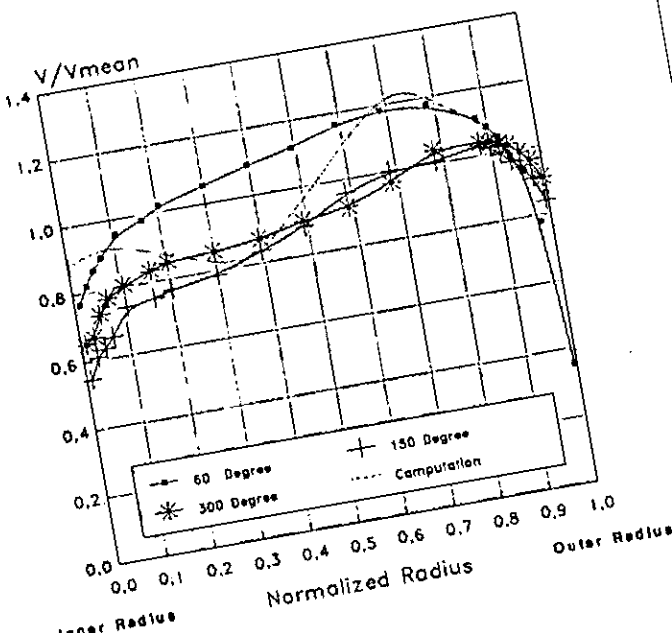

Fig. 7 Measured Velocity Distributions at Three Circumferential Positions of the Exit Plane